RSC Advances

PAPER

View Article Online
View Journal | View Issue

Cite this: *RSC Adv.*, 2023, **13**, 7300

A novel self-wrinkled polyurethane-acrylate wood coating with self-matting, anti-fingerprint performance and skin-tactile feeling *via* excimer lamp/UV curing

Yingchun Sun,[a] Jianfeng Xu,[a] Ling Long,[a] Jingya Gong,[a] Minggui Chen[b] and Ru Liu *[a]

Wrinkled surfaces exist widely in nature and organic living world, such as plants, insects, and skin. The optical, wettability and mechanical properties of materials can be enhanced by artificially preparing regular microstructure on the surface of materials. In this study, a novel self-wrinkled polyurethane-acrylate (PUA) wood coating with self-matting, anti-fingerprint performance and skin-tactile feeling curing by excimer lamp (EX) and ultraviolet (UV) was prepared. The wrinkles were formed on the surface of PUA coating at microscopic level after excimer and UV mercury lamp irradiation. The width and height of the wrinkles on the coating surface can be controlled to adjust the coating performance by changing the curing energy. When the PUA coating samples were cured by excimer lamp and UV mercury lamp with curing energy of 25–40 mJ cm^{-2} and 250–350 mJ cm^{-2}, the excellent coating performances were observed. The gloss value of self-wrinkled PUA coating at 20° and 60° were less than 3 GU, while at 85° was 6.5 GU, which satisfied the demanding of matting coating. Besides, the fingerprints on the coating samples could disappear in 30 s and could still have anti-fingerprint performance after 150 times of anti-fingerprint tests. Furthermore, the pencil hardness, abrasion quantity and adhesion of self-wrinkled PUA coating were 3H, 0.045 g and 0 grade respectively. Finally, the self-wrinkled PUA coating has excellent skin-tactile feeling for touching. The coating can be applied to wood substrates, and has potential application in the field of wood-based panels, furniture and leather.

Received 23rd February 2023
Accepted 26th February 2023

DOI: 10.1039/d3ra01220d

rsc.li/rsc-advances

1 Introduction

Wrinkled surfaces exist widely in nature and the organic living world, such as for plants, insects, and skin. The optical, wettability and mechanical properties of materials can be enhanced by artificially preparing a regular microstructure on the surface of materials.[1–3]

The preparation of a wrinkled surface can be divided into surface modification and self-organizing technology according to different preparation methods.[4–7] The former includes molding,[8] femtosecond laser[9] and photolithography.[10] The latter includes thermal expansion method,[11] phase separation method[12] and gradient curing method.[13] Burrell (1954) and his collaborators first artificially simulated the wrinkle process and preliminatively explained the wrinkle mechanism.[14] Later, on the basis of the work, a simple wrinkle model was summarized, namely the double-layer model.[15] With the expansion and deepening of research systems, such as the homogeneous system[16] and gradient system,[17] the two-layer theory has been further developed. Importantly, this advanced mechanical response mechanism can regulate the topography of the wrinkle, and then obtain the ordered structure of the wrinkle surface.

Compared with other wrinkled surface preparation methods, gradient curing method can prepare a large area self-wrinkled coating on the surface of a coating. Schubert *et al.* (2009) prepared the coating by two-step radiation method, and used low penetrating band and strong penetrating ultraviolet light to conduct gradient curing on the photocurable coating, forming a UV coating with wrinkle structure on the surface of the substrate.[18] Chandra and Crosby (2011) use the surface oxygen inhibition effect of acrylic crosslinking agent to cure acrylic coating directly in air environment by ultraviolet radiation. Due to the attenuation of light intensity from top to bottom, the gradient crosslinking density will be generated, which leads to the gradient physical property and thus produces the wrinkle structure.[19] At the same time, Tomes *et al.* (2012) used the surface enrichment characteristics of fluorinated catalyst to add the fluorinated catalyst into the photocurable coating.[20] Due to the large concentration of the surface catalyst, the difference of polymerization reaction rate up and down resulted in the complex shrinkage stress on the surface, which led to the

[a]*Research Institute of Wood Industry, Chinese Academy of Forestry, Haidian 100091, Beijing, China. E-mail: liuru@criwi.org.cn*
[b]*Jiangsu Haitian Technology Co., Ltd, Jurong 212400, Nanjing, China*

surface instability and prepared the surface wrinkle structure. All the above studies indicate that gradient curing is an effective method to prepare wrinkled structures of coatings.

Excimer lamp (EX) curing technology is an important radiation curing technology with many advantages, such as the low energy loss and high efficiency.[21–24] It is a very potential new environmental protection and energy saving curing technology. Naganuma *et al.* (2013) prepared PET/silicon coating containing SiO_2 by excimer lamp curing at low temperature. The experimental results showed that the coating had good adhesion, high surface hardness, and elastic modulus.[25] Ohishi *et al.* (2017) investigated the effect of excimer light irradiation on polysilazane coatings formed on PET films with vacuum-evaporated SiO_2 coatings.[26] The experimental results show that excimer lamp irradiation improved the compactness of the coating and reduced the water vapor permeability. Thus, the coating had excellent transparency and ductility and can be used in flexible electronic materials. However, due to the limitation of wavelength at 172 nm by the excimer lamp, only 0.1 μm depth of coating was cured completely, while the deeper is still not cured.[27–30] It is very suitable for the preparation of gradient curing self-wrinkled coatings because of the low penetration depth and high surface energy of excimer lamps. By this way, micro-wrinkles may exist on the cured coating surface.

After a series of studies, the self-wrinkled coating has the functions of matting, anti-fingerprint and low friction coefficient. Surface wrinkles not only improve the performance of coating, but also give coating more special functions and wider application potential. Calvez *et al.* (2022) studied the phase separation of a ternary mixture (PBGMA) consisting of polybutadiene polybutadiene diacrylate (PBUDA), cycloaliphatic diepoxide (CE) and hexadiol dimethacrylate (HDDMA).[31] The mixture is separated by a ternary phase and subjected to UV curing to form a matting coating with a self-wrinkled surface. Similarly, Zhang *et al.* (2022) prepared a gloss controlled UV-curable matting self-wrinkled waterborne urethane acrylate coating by controlling the number and depth of folds by adjusting the amount of photoinitiator added.[32] The results showed that the lowest gloss of the cured self-wrinkled coating could reach 5 GU, and the coating had good mechanical properties and hydrophobic properties.[32] Bian *et al.* (2022) also prepared a UV-curable anti-fingerprint coating based on epoxy resin for self-folding surfaces.[33] The results showed that the coating remained stable at the temperature of 352.2–364.8 °C, the water contact angle of the coating was between 103 and 105°, and the surface energy of the cured film was 24.58–20.69 mN m^{-1}. The coating had good thermal stability, anti-fingerprint performance and low surface energy. Some researchers had also studied the relationship between self-wrinkled surface coatings and their surface friction coefficient. Suzuki *et al.* (2016) used a relatively rigid film to prepare a coated surface with a wrinkled structure on the surface of a soft elastic fabric.[34] The results showed that the friction coefficient of fabric surface decreased significantly, and the friction coefficient of fabric surface is less than 0.1. The surface of the fabric had formed a smooth feeling of the skin-tactile feeling.

Traditional wrinkled surface processing technology is too expensive and it can only be used with small area and high value-added products such as optical lenses. However, normal UV-curable coatings can't be used for the preparation of wrinkled surface coatings. Therefore, it is a significant challenge to prepare a simple, fast and low-cost self-wrinkled coating with large-area.

At present, there are still very few related studies on excimer lamp curing self-wrinkled coating, and the influence of excimer lamp curing energy on the surface of self-wrinkled coating. In this work, we synthesized a series of self-matting, anti-fingerprint performance and skin-tactile feeling PUA wood coating with self-wrinkled surface curing by excimer lamp and mercury lamp. The coating performance was enhanced by wrinkles of coating surface and can prepare the large-scale size coatings on the wood substrate. Besides, the preparation process of self-wrinkled PUA coating was simple, convenient and eco-friendly. In addition, the self-matting, anti-fingerprint and skin-tactile feeling performance of self-wrinkled PUA coating were tested by coating surface characterization. The surface morphology and self-wrinkle mechanism were investigated by FTIR, XPS, UDM, AFM.

2 Materials and methods

2.1 Materials

The monomers of trimethylolpropane triacrylate (TMPTA), 1,3-butanediol diacrylate (BDA), 2-hydroxyethyl acrylate (HEA) with AR level were purchased from Shanghai Hechuang Chemical Technology Co. Ltd, Shanghai, China. The photoinitiator of benzophenone (BP) was purchased from McLean Biochemical Technology Co. Ltd, Beijing, China. Two types of oil-based polyurethanes with two terminal –NCO groups (synthesized by isophorone diisocyanate and polyethylene glycol-200, labeled as PU2) and three terminal –NCO groups (synthesized by isophorone diisocyanate, polyethylene glycol-400, and glycol, labeled as PU3) were obtained from Jiangsu Himonia Technical Co. Ltd, Zhenjiang, China. The dispersant labeled BYK-180 was purchased from BYK Additives (Shanghai) Co. Ltd, Shanghai, China. The filler powder (SiO_2, 3 μm) labeled OK412 was purchased from Degussa (Shanghai) Co. Ltd, Shanghai, China. The melamine-urea (MF) resin impregnated paper decorated particleboard with dimension of 2440 mm × 1220 mm × 18 mm (thickness) were provided by Suofeiya Home Collection Co. Ltd, China. The distilled water in this study was prepared in the laboratory. All the materials were utilized as received without purification.

2.2 Synthesis of the PUA wood coating

The formulas of PUA wood coatings were following Table 1. The synthesis of skin-tactile coating was carried out in a three-neck flask by water bath. 28 g TMPTA, 20 g BDA, 10 g HEA, and 6 g benzophenone were pre-dispersed at 700 rpm for 30 min. After heating up to 70 °C, 10 g PU2, 20 g PU3, and 2 g BYK180 were added into the flask and remained for 30 min. Afterwards, the reaction was cooled down to 50 °C, and 10 g OK412 was added

Table 1 Proportions of PUA wood coatings

	Monomer			Oligomer		Coating additive	Photoinitiator	Filler
	TMPTA	HEA	BDA	PU2	PU3	BYK-180	BP	OK412
Composition proportion (wt%)	28	10	20	10	20	4	6	2

into the flask and stirred at 1000 rpm for 40 min. The coating was obtained after filtering by a filter bag at 100-mesh. The synthesis procedure was shown in Fig. 1. The OK412 in the coating was used as a wear-resistant filler, not a matting agent.

2.3 Preparation of self-wrinkled PUA coating

The preparation of self-wrinkled PUA coating was shown in Fig. 2. The PUA wood coating was coated on the MF resin impregnated paper decorated particleboard (2440 mm × 1220 mm × 18 mm) by roll-coated method. Afterwards, the thickness of wet coating was about 60 μm (measured by CT638 film thickness gauge, Three quantity, Dongguan, China). The PUA coating samples were cured by 172 nm excimer lamp (PRT-L2, Foshan Shunde PURETE Mechanical Co., Ltd) and UV mercury lamp (PRT-1320, Foshan Shunde PURETE Mechanical Co., Ltd) with different UV curing energy for 10 s.

The self-wrinkled PUA cured coating films were obtained by above steps. The control sample labeled as C_1 was only cured by UV mercury lamp with the curing energy of 250–350 mJ cm^{-2}. The smooth sample which was labeled as C_2 was pre-cured by 172 nm excimer lamp (under the protection of nitrogen, the oxygen concentration was lower than 100 ppm) with curing energy of 5–15 mJ cm^{-2} (measured by LS131 UV energy meter, Linshang, Shenzhen, China) and completely cured by UV mercury lamp with curing energy of 250–350 mJ cm^{-2}. The matting sample labeled as C_3 was pre-cured by 172 nm excimer

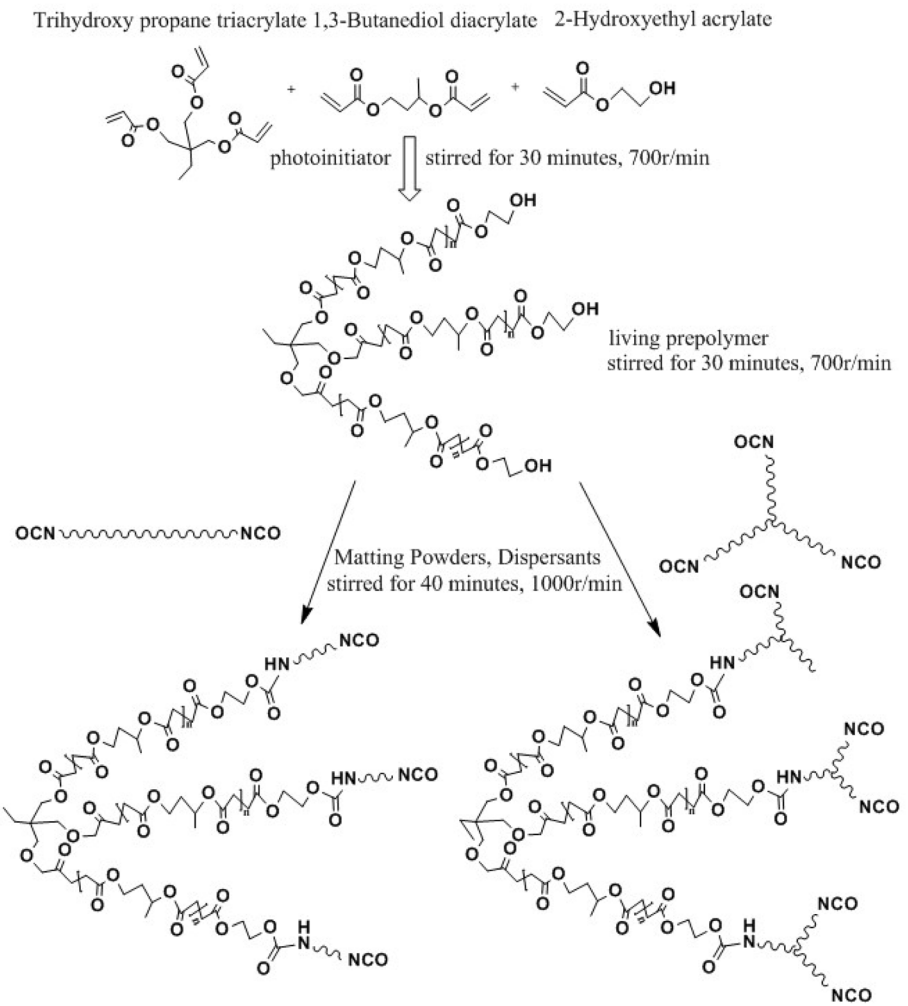

Fig. 1 Synthesis of the PUA wood coating.

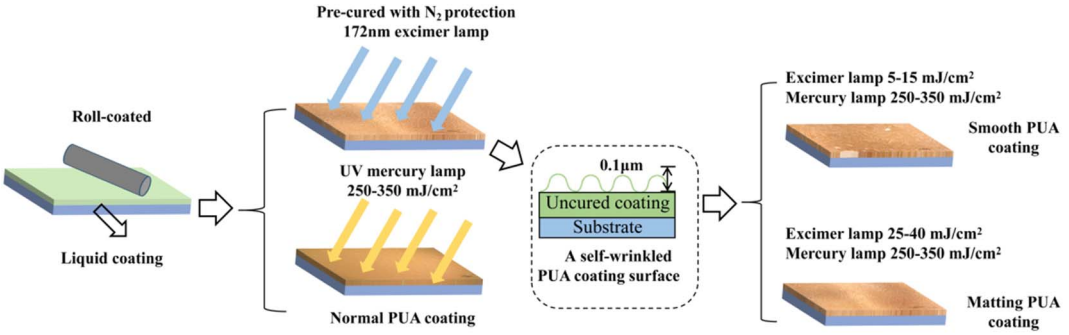

Fig. 2 Preparation of self-wrinkled PUA coating.

lamp with curing energy of 25–40 mJ cm^{-2} and completely cured by UV mercury lamp with curing energy of 250–350 mJ cm^{-2}. Each group of the samples were made with three replicates for calculated the average and standard deviation values. The preparation method of self-wrinkled PUA wood films were following Table 2.

2.4 Characterizations

2.4.1 Surface chemical characterization. The surface chemical structure and compositions of self-wrinkled PUA cured coating films were characterized on an FTIR spectrometer (VERTEX 80V, Bruker Daltonics technology Company, Berlin, Germany) and an XPS spectrometer (ESCALAB 250Xi, Thermo Fisher Scientific, Waltham, USA). The FTIR analyses were carried out on the coating surfaces with testing area of 1 mm × 1 mm. The XPS analyses were carried out to determine the functional groups present on the coating surface with a pass energy of 10 eV and nonmonochromatic MgKα and AlKα X-radiations. The samples with testing area of 4 mm × 4 mm were mounted onto a holder attached by double-sided adhesive tape and placed in vacuum.

2.4.2 Surface morphology characterization. The macro-morphology and roughness of the samples were observed by UDM (MSD-VHX1000, Keyence, Japan) in the transmission mode. The nano-morphology of the coating was characterized by AFM (Dimension Edge, Bruker, USA) which was collected by a scanning probe microscope in contact mode with testing area of 2 μm × 2 μm. The S_a (surface arithmetic mean deviation) and S_q (surface root mean square deviation) of the coating samples were measured by image processing software SPI3800N and according to the international standard ISO 25178-2-2021. The S_a and S_q were calculated using eqn (1) and (2):

$$S_a = (1/NM)\sum_{i=1}^{N}\sum_{j=1}^{M}|Z_{ij}| \quad (1)$$

$$S_q = \sqrt{\frac{1}{MN}\sum\sum Z(x,y)^2} \quad (2)$$

where Z is the distance from the point on the contour of the object surface area to the reference plane, and M and N are the sampling points in two directions perpendicular to each other in the evaluation area.

2.4.3 Physical and mechanical characterization

2.4.3.1 Gloss. The gloss value of the cured coating samples were measured by an WGG60-E4 gloss meter (Keshijia, Quanzhou, China) at an incident angle of 60°, which according to the Chinese standard of GB/T 9754-2007. During the test, three difference places of the same sample were measured and the average value was calculated.

2.4.3.2 Mechanical property. The resistance abrasion property of cured coating samples were ground by a Taber-type abrasion tester (TST-C1020, TST Instruments, Quanzhou, China) with a load of 500 g taped 180-mesh sandpapers for 100 revolutions of abrasion. The abrasion quality of cured coating samples were measured before and after grounding according to the Chinese standard of GB/T 15036-2018. The hardness of the coatings was tested by a car pencil hardness tester (BY-500 g, Pushen, Shanghai, China) according to the Chinese standard of GB/T 6739-2006. A force of 7.5 kg m s^{-2} for the tip of the pencil was applied on the surface at an angle of 45°, the coated samples were pressed by the pencils until the surface was damaged by 3 mm scratch. The results were determined by the lower level hardness of the pencil when damage occurred. The adhesion of cured coating films were measured by a BYK5125 cross-cut tester (BYK, Berlin, Germany) at gap of 2 mm,

Table 2 Preparation method of self-wrinkled PUA coating

Coating	Excimer lamp (mJ cm^{-2})	UV mercury lamp (mJ cm^{-2})	Coating thickness (μm)	Curing time (s)
C_1	0	250–300	60	10
C_2	5–15	250–300	60	10
C_3	25–40	250–300	60	10

according to the Chinese standard of GB/T 9286-2021. The grade based on detached area of the coatings from the wood substrate was used to determine the adhesion properties, where grade 0 was the best, and the adhesion of grade 5 was the worst.

2.4.3.3 Anti-fingerprint performance and water contact angle. The process of anti-fingerprint performance testing was determined as follows: The hands were washed with clean water, and dried with a clean towel. After air-dried (without touching anything) for 1 minute, the surface of the coated particleboard was pressed with one finger at approximate 10 N. Then, the finger was removed, and the disappearance of fingerprints was observed with recording of time, each group was repeated for 6 times. Meanwhile, the contact angles of the samples by finger-wipe tests were recorded after every fifty times. The water contact angle of self-wrinkled PUA coatings samples were measured for six times with deionized water (7 μL) in different places employing Contact Angle System (Data Physics, Germany). The average values from three parallel measurements were reported.

2.4.4 Skin-tactile feeling characterization. The skin-tactile feeling of the cured coating samples were evaluated by questionnaire adjustment of 50 testers including 25 males and 25 females.[35] The average age of the testers was 24 years ranging from 20 to 30 years of age. All the participating testers were right-handed and native speakers of Chinese and had normal or corrected to normal vision, normal hearing without any psychiatric diseases. The testers gently touched the surface of the panels with the right hand and judged the feeling of surface into 5 grades, namely, 1-uncomfortable, 2-fairly uncomfortable, 3-neutral, 4-fairly comfortable, and 5-comfortable. The numbers of testers and the grades were collected.

3 Results and discussion

3.1 Surface chemical analysis

Fig. 3 shows the FTIR-ATR spectra of self-wrinkled PUA coating cured by different curing methods. The bands at 2920, 1724 and 1094 cm^{-1} were the characteristics for the PUA coating.[36] The band at 2920 cm^{-1} was attributed to the vibration absorption of the $-CH_2-$ group and the band at approximately 1724 cm^{-1} was derived from C=O groups. The strong peak at 1094 cm^{-1} was the stretching vibration of C–O bond. The most difference between C_1 samples and C_2, C_3 samples were the absorption bands at 1448, 1246 and 742 cm^{-1}. The peaks at 1448 cm^{-1} and 742 cm^{-1} were assigned to the incompletely cured non-conjugated and conjugated vinyl groups, respectively in acrylates monomers. The significantly reduction of C_2 and C_3 groups in the two regions indicated the further curing of coatings pre-cured by excimer lamp. In the process of excimer lamp curing, the coating was protected by nitrogen, which effectively reduced the phenomenon of oxygen polymerization and made the surface of coating samples cure more completely. The peak at 1246 cm^{-1} was attributed to the vibration absorption of C–O bond. The shift of this peak to 1094 cm^{-1} suggested that after the excimer curing of the ester compound, a large number of monomers were polymerized to form a cross-linking structure. Besides, after combined curing, the peak at 1724 cm^{-1} (C=O) significantly weakened indicating that the coating cured by combined curing was more complete than UV curing. However, for the C_2 and C_3 groups, no much difference was found, suggesting the surface chemical structures were almost the same.

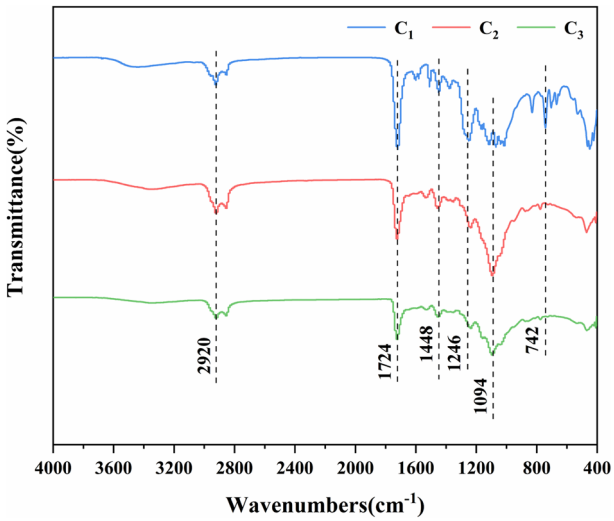

Fig. 3 FT-IR spectra of UV cured PUA coating (C_1) and self-wrinkled PUA coating (C_2, C_3).

The XPS spectra of self-wrinkled PUA coating under different curing methods were shown in Fig. 4. It can be clearly observed that peaks attribute to C1s, O1s in the Fig. 4(a). A small amount of nitrogen and silicon peaks may be caused by fillers in the coating preparation process. The C1s XPS spectra shown in Fig. 4(b) shows three peaks: the peak at 284.8 eV was assigned to the C–C bond, the peak at 286.3 eV correspond to C–O bond and the peak at 288.8 eV was attributed to the C=O bond. Compared with C_1, the coating samples cured by excimer lamp and UV mercury lamp was different from the coating samples cured only by UV. There was no change in C–C bond at 284.8 eV, but the peaks of C–O bond at 286.3 eV and C=O bond at 288.8 eV were significantly enhanced. The result indicated that the reaction of polyurethane acrylate monomer in the cross-linking curing process was more complete and the content of C–O, C=O bond were increased. The O1s XPS spectra shown in Fig. 4(c) also proved the phenomenon. The UV curing coating had only one peak at 532.28 eV assigned to C–O bond and the C_2 and C_3 coating samples have two peaks at 532.28 eV for C–O bond and 533.28 eV for C=O bond. After combined curing by excimer lamp and UV mercury lamp, the coating gradually produced C=O bond with the increasing of energy. As listed in Fig. 4(d), the content of C–C bond in C_2, C_3 coating samples was decreasing from 83.29% to 68.13% compared with the C_1 coating samples. In the meanwhile, the content of C–O and C=O bond were increasing from 3.75% to 8.64% and 12.96% to 23.23% respectively. The significant increase of C–O and C=O bond in the C_2 and C_3 groups indicated that the conversion rate of polyurethane acrylate monomer was increasing by pre-cured of excimer lamp. Compared with C_2 coating samples, the content of C–C bond in C_3 coating samples decreased from 69.79% to 68.13%. The content of C–O bond increases from

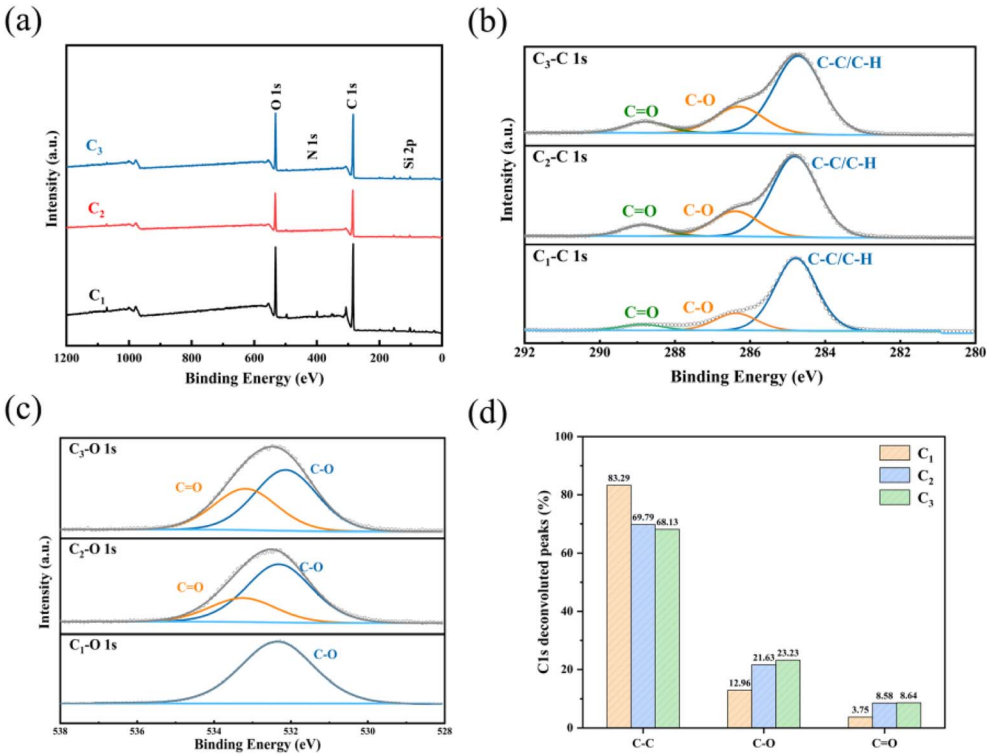

Fig. 4 XPS spectra of UV cured PUA coating (C_1) and self-wrinkled PUA coating (C_2, C_3) (a) full spectrum (b) C1s spectrum (c) O1s spectrum (d) C_{1s} deconvoluted peaks of C–C, C–O, C=O bond content of coating.

21.63% to 23.23% and the content of C=O also increased from 8.58% to 8.64%. The content differences between C_2 and C_3 coatings showed that the conversion rate of PUA coating samples can be controlled by adjusting curing energy and the increasing of curing energy can also increase the degree of polymerization crosslinking of the coating samples.[37–39]

3.2 Surface morphology, gloss and roughness

The surface morphologies of the C_1, C_2, C_3 coating samples were characterized by UDM and AFM respectively, the results were shown in Fig. 5. The UDM and AFM observations in Fig. 5(a) revealed that the surface of C_1 PUA coating samples were smooth but had a few shrinkage holes, which may be caused by oxygen resistance during the curing process. In the meanwhile, the surface morphologies of the C_2, C_3 coating samples were shown in Fig. 5(b) and (c). From Fig. 5(b) and (c), it can be clearly observed that few wrinkles appeared on the surface of the coating samples. The width of wrinkles on the surface of C_2 coating samples was about 7.5–9 μm and the wrinkle width of C_3 coating samples was increasing significantly which reached 11–13 μm. This indicated that the surface of the coating pre-cured by excimer lamp had self-wrinkled phenomenon.[40] With the increasing of curing energy, the width and number of wrinkles on the surface of coating samples were also increased. The results proved that the precuring and curing energy of excimer lamp played a very important role in the curing process of coating. In order to assess the relationship between the morphology of the coating surface wrinkles and the curing energy, AFM imaging was performed at multiple locations across the sample. It was shown in Fig. 5, the apparent wrinkles height of C_1 coating was found to be 92.9 nm, and the height of C_2, C_3 coating were 119.1 and 355.8 nm. The wrinkles height of C_2, C_3 coating samples was increasing after pre-cured by excimer lamp, which was in good agreement with UDM results. After excimer lamp precuring and UV mercury lamp curing, the surface of the coating formed a self-wrinkled structure. The width and height of the wrinkles was increasing with the increase of curing energy, which affected the morphology of the coating surface. The results of the coating surface topography were in good agreement with the results of the study by Bauer *et al.*,[41] who also observed wrinkled surface microstructures cured by excimer lamp.

The gloss value and roughness of the C_1, C_2, C_3 coating samples were characterized respectively, the results was shown in Fig. 6. As shown in Fig. 6(a), with the incidence angle of 20°, 60° and 85°, the gloss value differ significantly. The gloss value of C_1 coating sample was higher than C_2, C_3 coating samples. When the incidence angle was 20° and 60°, the gloss value of C_1 was 15.5 and 26.6 GU. However, the gloss value of C_2, C_3 were less than 3.0 GU, which was satisfying the demanding of matte coating. The gloss value of 85° incidence angle was a key feature for judging matte coating film. When the incidence angle was 85°, the gloss value of C_1, C_2, C_3 were 51.4 GU, 7.7 GU and 6.5 GU respectively. The difference between treatment with excimer lamp and without excimer lamp was obviously. It was clearly shown from the results that there was a strong relationship

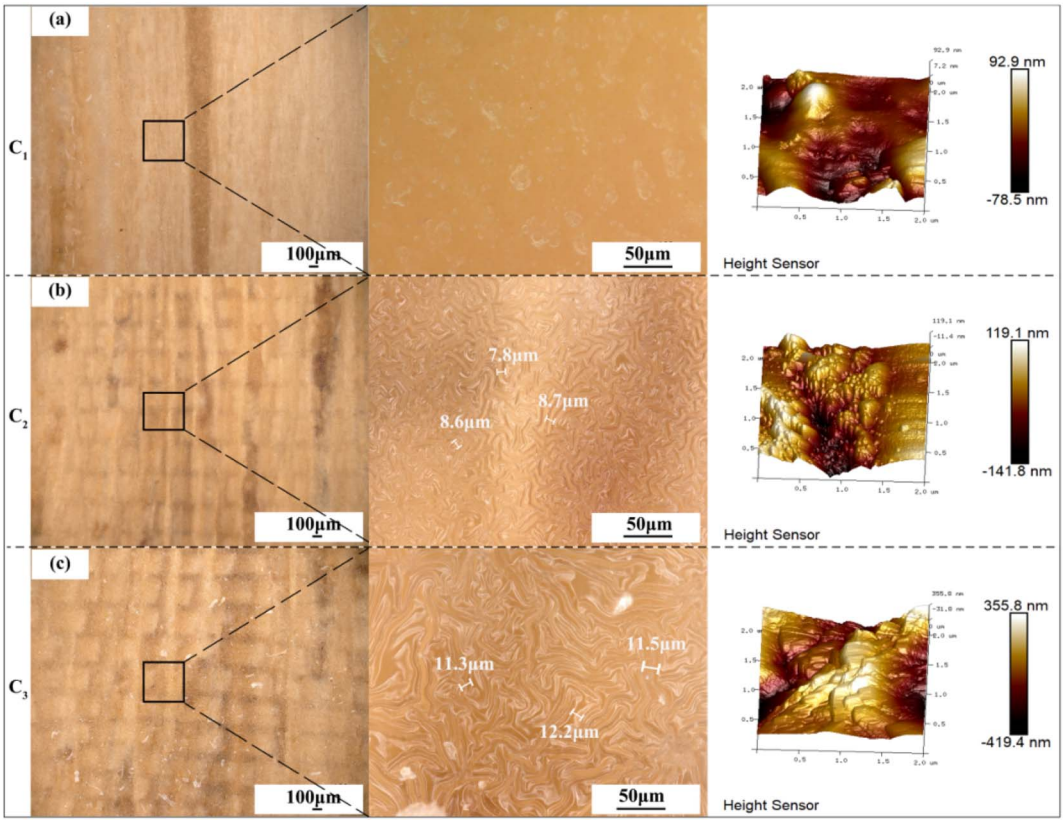

Fig. 5 UDM and AFM images of PUA self-wrinkled coatings for (a) C_1 (b) C_2 (c) C_3.

between the change of gloss value and the structure of coating surface. The roughness of C_1, C_2, C_3 were shown in Fig. 6(b), the S_a and S_q of C_1 coating samples were only 0.09 μm and 0.15 μm, while the gloss value at 85° was 51.4 GU. This showed that the existence of wrinkles was an important factor in matte coating. With the increase of curing energy, the width and height of the surface wrinkles was increasing, and the gloss value of the coating decreased. The S_a and S_q of C_2, C_3 coating samples were 0.3 μm, 0.5 μm and 0.6 μm, 0.8 μm. This indicated that the micro-wrinkles structure of the coating surface showed matte coating performance. The height and width of the wrinkles in C_3 are higher than those in C_2, and the light incident on the coating wrinkles surface would be reflected and absorbed between the wrinkles. So less light was reflected back to the glossometer, resulting in a lower gloss value for C_3 than C_2.

As a result, the addition of excimer lamp curing and the change of curing energy play an important role in the formation of wrinkles and matte properties on the coating surface. The curing depth of excimer lamp was lower than 0.1 μm, when the coating samples was curing by excimer lamp, the liquid

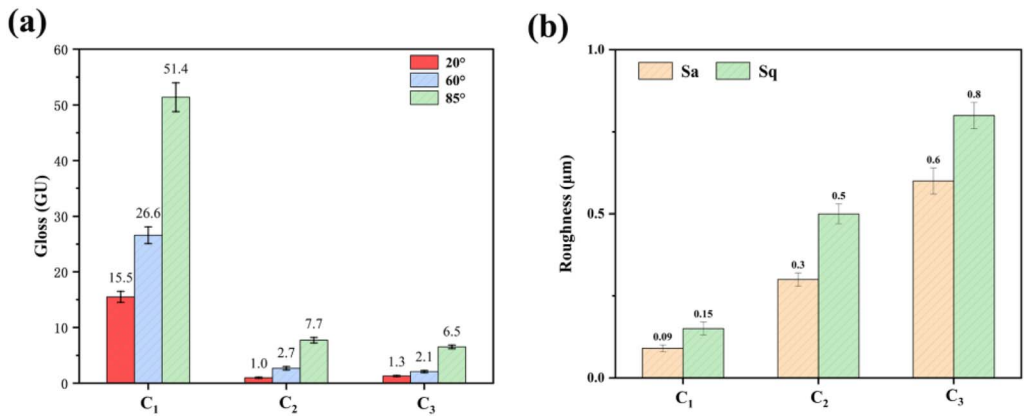

Fig. 6 The (a) gloss value (at 20°, 60° and 85°) and (b) roughness of C_1, C_2, C_3 coating samples.

coatings form two different layers. Due to the low penetration but high energy of the excimer lamp, the irradiated coating surface began to cure and wrinkles formed in the top layer of the coating due to uneven internal stresses. However, the bottom of the coating was still liquid statement. After UV mercury lamp curing, the coating was completely cured and the wrinkles on the coating surface was remained. The wrinkles and roughness of the coating surface affected the matte performance of the coating and the self-wrinkled PUA coating cured by excimer lamp and mercury lamp had good matte performance. The coating samples had only 6.5 GU at 85° incidence angle.

3.3 The physical performance of self-wrinkled PUA coating

The physical performance of self-wrinkled coatings under different curing methods are listed in Fig. 7. As shown in Fig. 7(a), the pencil hardness and abrasion quantity of C_1, C_2, C_3 coating samples were characterized by physical tests to explore the physical performance of the coating surface. The pencil hardness of C_1 was H, while C_2 and C_3 had pencil hardness of 2H, 3H, which was attributed to the dual UV curing process, which was not only created a wrinkled structure on the coating surface but also improved the curing degree of the coating samples. For the abrasion performance of coating samples, the abrasion quantity of C_1 was much higher than C_2 and C_3, which were 0.100 g, 0.071 g and 0.045 g respectively. When the curing energy of excimer lamp increased, the wrinkles and abrasion resistance of the coating are further increased. The results showed that the generation of wrinkles enhanced the abrasion resistance of the coating and the result showed that the generation of wrinkles could enhance the mechanical properties of the coating, and the mechanical properties was improved with the increase of the width and height of the wrinkles. In terms of coating adhesion in Fig. 7(b), the C_1 groups were worse than C_2 and C_3 groups, which only had 2 grade. After curing by excimer lamp and UV mercury lamp, the adhesion of C_2 and C_3 groups were significantly improved to 0 grade. Above all, the results showed that the curing methods and energy had a significant effect on the physical performance of the coating.

3.4 The anti-fingerprint performance and water contact angle

The result of anti-fingerprint performance testing of self-wrinkled coatings under three types of curing methods after 1 s (a, b, c) and 1 min (a′, b′, c′) was shown in Fig. 8. Compared with the C_1 samples, the fingerprints on the coating samples of the C_2 and C_3 samples could almost disappear, while the fingerprints and water spots on the coating of the control samples couldn't completely disappear. The fingerprints on C_2 was disappeared completely after 60 s of hand contact, while The fingerprints disappeared on C_3 was shorter, with an average of 30 s. The C_1 coating samples were only curing by UV mercury lamp and didn't have wrinkles on the coating surface. This indicated that wrinkles on the coating surface paly a important role in the coating performance of anti-fingerprint.[42] Fingerprints were composed of a mixture of liquid and grease on the hand, which can easily leave fingerprints on the surface of normal materials.[43,44] The surface of the self-wrinkled coating had a wrinkle-like texture. When the fingerprint was on the surface of the coating, it would produce an extension effect due to the gullies composed of the wrinkles, which showed the disappearance of the fingerprint on the macroscopic level. In order to further study the anti-fingerprint performance of the coating, the anti-fingerprint durability (Fig. 8(d)) and water contact angle (Fig. 8(e)) of the coating were tested. Through the durability test of the coating, it was found that the water contact angle of C_1 increased from 64.4° to 80° after 150 times of durability test, and the coating didn't have anti-fingerprint performance. The surfaces of C_2 and C_3 coatings showed hydrophilicity, which was consistent with the results of fingerprint resistance tests. After 100 times of finger-wipe test, the water contact angle of C_2 was increasing from 36.6° to 57°.

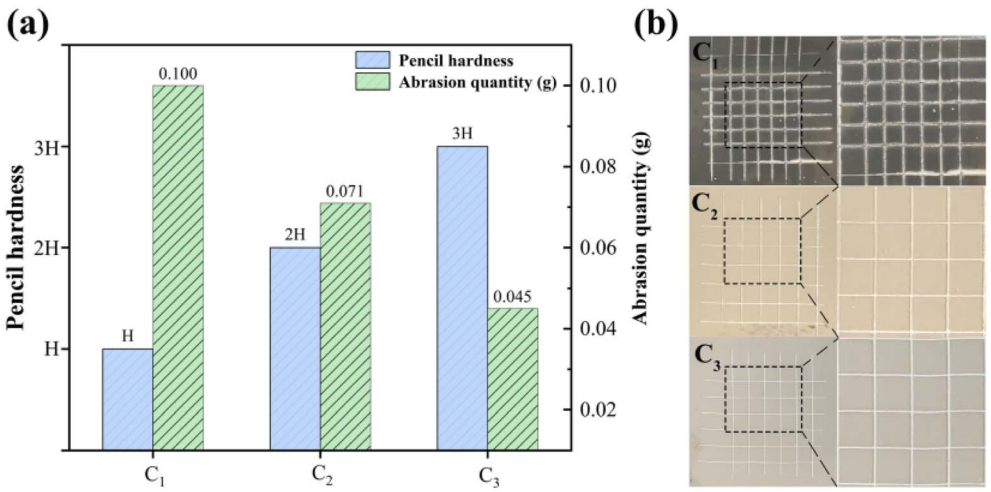

Fig. 7 (a) The pencil hardness and abrasion quantity of C_1, C_2, C_3 coating samples; (b) the digital photos of C_1, C_2, C_3 coating samples after cross-cut adhesion test.

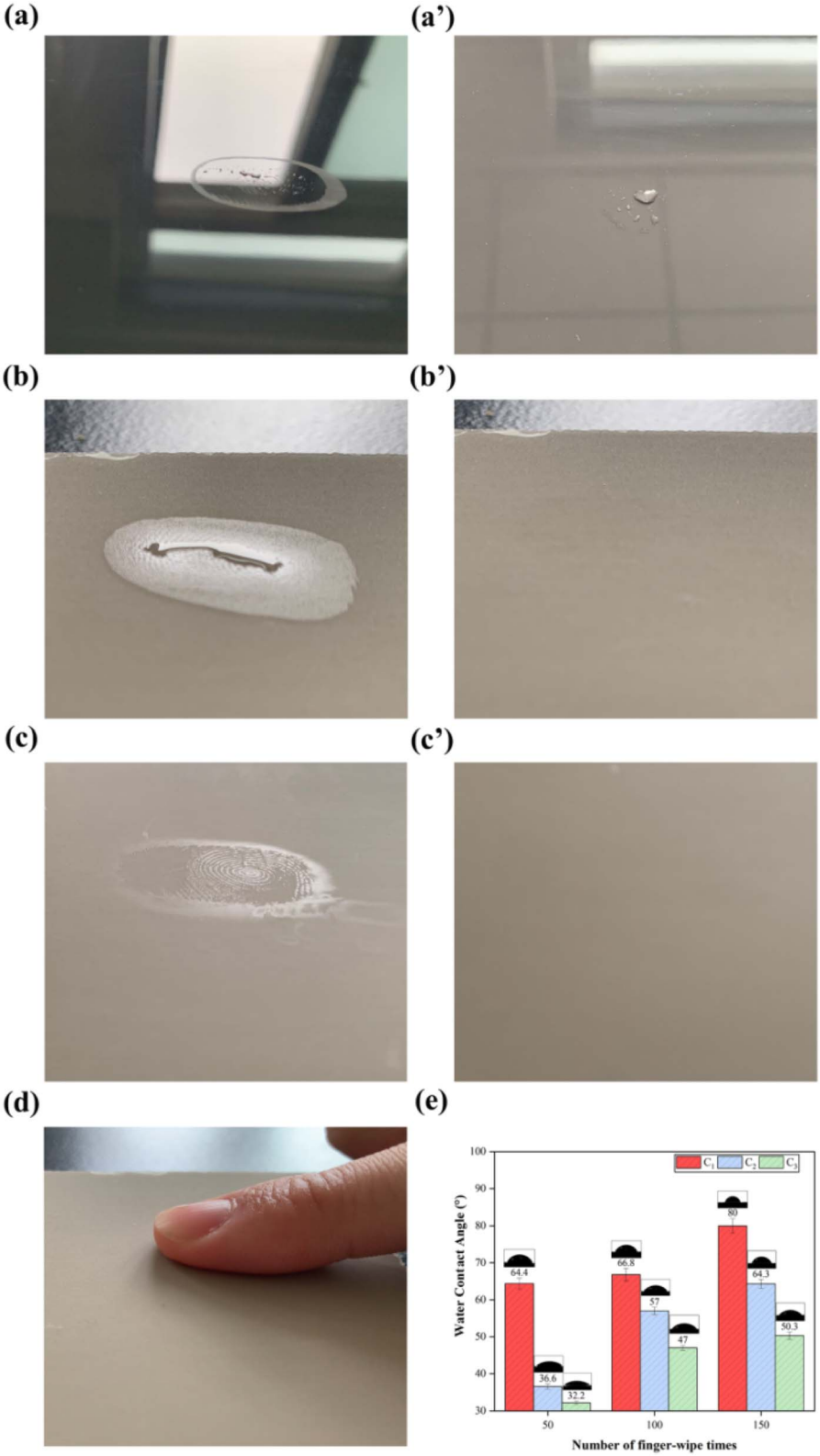

Fig. 8 Anti-finger test images of PUA self-wrinkled coating samples after 1 s (a) C_1 (b) C_2 (c) C_3 and 1 min (a′) C_1 (b′) C_2 (c′) C_3. (d) The image of finger-wipe test. (e) The water contact angle of self-wrinkled coating surfaces after finger-wipe tests.

Furthermore, the water contact angle of C_2 was increasing from 57° to 64.3°. The water contact angle of C_2 was increasing from 32.2° to 50.3° after 150 times of finger-wipe test. This indicated that the wrinkle structure of the surface of the self-wrinkle coating played a role in anti-fingerprint performance. With the increasing of durability times, the wrinkle structure of the

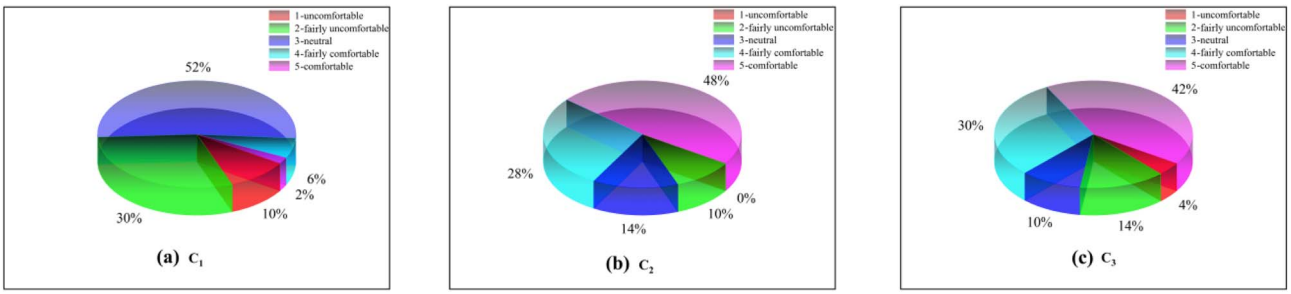

Fig. 9 Skin-tactile performance test of PUA self-wrinkled coatings with different curing method. (a) C_1, (b) C_2, (c) C_3.

coating had a slight damage, but it still had excellent anti-fingerprinting performance.

3.5 Skin-tactile performance of coatings

The result of skin-tactile performance test of coatings for skin-tactile coatings with three types of curing methods was shown in Fig. 9. There were 50 testers including 25 males and 25 females taking the test and scoring the surface feeling of the three types of samples. The testers gently touched the surface of the panels with the right hand and judged the feeling of surface into 5 grades, namely, 1-uncomfortable, 2-fairly uncomfortable, 3-neutral, 4-fairly comfortable, and 5-comfortable. The numbers of testers and the grades were collected to evaluate the skin-tactile performance of the coating surface by the comprehensive grades. As seen from Fig. 9, the feeling of 50 testers for touching the surface of coating changed significantly after combined curing. More than half of the testers thought the UV-cured coatings had feelings of neutral and only 2% think the surface was comfortable, while the C_2 and C_3 coatings had big improvements in comfortable feelings, where the C_2 and C_3 were increased to 48% and 42%. The results showed that both the C_2 and C_3 coating samples may make people feel comfortable.

4 Conclusion

In this research, a novel self-wrinkled polyurethane-acrylate wood coating with self-matting, anti-fingerprint performance and skin-tactile feeling curing by excimer lamp and UV mercury lamp was prepared, and applied on the impregnated paper decorated particleboard. This method is simple, convenient and eco-friendly, which can easily prepare large scale wood coating with self-matting, anti-fingerprint and skin-tactile feeling surface. After mercury and excimer lamp irradiation, the wrinkles were formed on the surface of PUA coating at microscopic level. By changing the curing energy, the width and height of the wrinkles on the coating surface can be controlled to adjust the coating performance. When the PUA coating samples were cured by 172 nm excimer lamp with curing energy of 25–40 mJ cm^{-2} and UV mercury lamp with curing energy of 250–350 mJ cm^{-2}, the excellent coating performances were observed. The gloss value of self-wrinkled PUA coating at 20° and 60° were less than 3 GU, while at 85° was 6.5 GU, which satisfied the demanding of matting coating. Furthermore, the pencil hardness, abrasion quantity and adhesion of self-wrinkled PUA coating were 3H, 0.045 g and 0 grade respectively, which were better than normal UV curable PUA coating. Besides, the fingerprints on the coating samples could disappear in 30 s and could still have anti-fingerprint performance after 150 times of anti-fingerprint tests. In addition, the self-wrinkled PUA coating has excellent skin-tactile feeling for touching. Thus, the self-wrinkled PUA wood coating have great potential for practical applications in wood-based panels, furniture and leather fields.

Conflicts of interest

The authors declare that they have no conflict of interest.

Acknowledgements

National key research and development project 2022YFD2200703.

References

1 Y. Zhang, D. Yao, S. Wang, Z. Xiao and X. Yu, Large-scale fabrication of waterborne superamphiphobic coatings for flexible applications, *RSC Adv.*, 2018, **8**, 36375–36382.
2 P. Liu, J. Zhu, L. Cheng, X. Liu and R. Liu, Curing and properties of urethane acrylates with different functionalities under electron-beam and ultraviolet irradiation, *Prog. Org. Coat.*, 2021, **156**, 106252.
3 Z. Lin, Z. Sun, C. Xu, A. Zhang, J. Xiang and H. Fan, A self-matting waterborne polyurethane coating with admirable abrasion-resistance, *RSC Adv.*, 2021, **11**, 27620–27626.
4 Q. Yong, D. Xu, Q. Liu, Y. Xiao and D. Wei, Advances in polymer-based matte coatings: A review, *Polym. Adv. Technol.*, 2022, **33**, 5–19.
5 T. Zhu, C. Jiang, M. Wang, C. Zhu, N. Zhao and J. Xu, Skin-Inspired Double-Hydrophobic-Coating Encapsulated Hydrogels with Enhanced Water Retention Capacity, *Adv. Funct. Mater.*, 2021, **31**, 2102433.
6 J. L. Yong, Y. La, O. S. Jeon, H. J. Lee and Y. P. Sang, Effects of boron nitride nanotube content on waterborne polyurethane–acrylate composite coating materials, *RSC Adv.*, 2021, **11**, 12748–12756.

7 J. Wang, X. Wu, Y. Wang, W. Zhao, Y. Zhao, M. Zhou, Y. Wu and G. Ji, Green, Sustainable Architectural Bamboo with High Light Transmission and Excellent Electromagnetic Shielding as a Candidate for Energy-Saving Buildings, *Nano-Micro Lett.*, 2023, **15**, 11.
8 Y. Li, J. John, K. W. Kolewe, J. D. Schiffman and K. R. Carter, Scaling up nature: large area flexible biomimetic surfaces, *ACS Appl. Mater. Interfaces*, 2015, **7**, 23439–23444.
9 J. Yong, F. Chen, Q. Yang, G. Du, H. Bian, D. Zhang, J. Si, F. Yun and X. Hou, Rapid fabrication of large-area concave microlens arrays on PDMS by a femtosecond laser, *ACS Appl. Mater. Interfaces*, 2013, **5**, 9382–9385.
10 P. Hartsuch, *Chemistry of Lithography*, Lithographic Technical Foundation, New York, 1961.
11 C.-M. Chen and S. Yang, Wrinkling instabilities in polymer films and their applications, *Polym. Int.*, 2012, **61**, 1041–1047.
12 Q. Yong, F. Nian, B. Liao, Y. Guo, L. Huang, L. Wang and H. Pang, Synthesis and surface analysis of self-matt coating based on waterborne polyurethane resin and study on the matt mechanism, *Polym. Bull.*, 2017, **74**, 1061–1076.
13 M. Guvendiren, S. Yang and J. A. Burdick, Swelling-induced surface patterns in hydrogels with gradient crosslinking density, *Adv. Funct. Mater.*, 2009, **19**, 3038–3045.
14 H. Burrell, High polymer theory of the wrinkle phenomenon, *Ind. Eng. Chem.*, 1954, **46**, 2233–2237.
15 N. Bowden, S. Brittain, A. G. Evans, J. W. Hutchinson and G. M. Whitesides, Spontaneous formation of ordered structures in thin films of metals supported on an elastomeric polymer, *Nature*, 1998, **393**, 146–149.
16 J. Groenewold, Wrinkling of plates coupled with soft elastic media, *Phys. A*, 2001, **298**, 32–45.
17 E. S. Matsuo and T. Tanaka, Patterns in shrinking gels, *Nature*, 1992, **358**, 482–485.
18 R. Schubert, T. Scherzer, M. Hinkefuss, B. Marquardt, J. Vogel and M. R. Buchmeiser, UV-induced micro-folding of acrylate-based coatings, *Surf. Coat. Technol.*, 2009, **203**, 1844–1849.
19 D. Chandra and A. J. Crosby, Self-wrinkling of UV-cured polymer films, *Adv. Mater.*, 2011, **23**, 3441–3445.
20 J. M. Torres, C. M. Stafford and B. D. Vogt, Photoinitiator surface segregation induced instabilities from polymerization of a liquid coating on a rigid substrate, *Soft Matter*, 2012, **8**, 5225.
21 I. Calvez, C. R. Szczepanski and V. Landry, Preparation and characterization of low gloss UV-curable coatings based on silica surface modification using an acrylate monomer, *Prog. Org. Coat.*, 2021, **158**, 106369.
22 T. Xie, W. Kao, Z. Zhang, Y. Liu and Z. Li, Synthesis and characterization of organosilicon modified self-matting acrylate polymer: insight into surface roughness and microphase separation behavior, *Prog. Org. Coat.*, 2021, **157**, 106300.
23 I. M. Mousaa, N. M. Ali and M. K. Attia, Preparation of high performance coating films based on urethane acrylate oligomer and liquid silicone rubber for corrosion protection of mild steel using electron beam radiation, *Prog. Org. Coat.*, 2021, **155**, 106222.
24 J. Franke, T. Koutecký and M. Malý, Study of process parameters of the atomizer-based spray gun for the application of a temporary matte coating for 3D scanning purposes, *Mater. Chem. Phys.*, 2022, **282**, 125950.
25 Y. Naganuma, T. Horiuchi, C. Kato and S. Tanaka, Low-temperature synthesis of silica coating on a poly(ethylene terephthalate) film from perhydropolysilazane using vacuum ultraviolet light irradiation, *Surf. Coat. Technol.*, 2013, **225**, 40–46.
26 T. Ohishi and Y. Yamazaki, Formation and Gas Barrier Characteristics of Polysilazane-Derived Silica Coatings Formed by Excimer Light Irradiation on PET Films with Vacuum Evaporated Silica Coatings, *Mater. Sci. Appl.*, 2017, **08**, 1–14.
27 S. Periyasamy, M. L. Gulrajani and D. Gupta, Preparation of a multifunctional mulberry silk fabric having hydrophobic and hydrophilic surfaces using VUV excimer lamp, *Surf. Coat. Technol.*, 2007, **201**, 7286–7291.
28 S. S. Song and G. J. Zhao, Expression of physiological sensation of anatomical patterns in wood: an event-related brain potential study, *BioResources*, 2012, **7**, 5593–5610.
29 Z. Lin, Z. Sun, C. Xu, A. Zhang, J. Xiang and H. Fan, A self-matting waterborne polyurethane coating with admirable abrasion-resistance, *RSC Adv.*, 2021, **11**, 27620–27626.
30 K. Wang, J. Cheng, Y. Zhu, X. Wang and X. Li, Experimental research on the performance of the thermal-reflective coatings with liquid silicone rubber for pavement applications, *e-Polym.*, 2021, **21**, 453–465.
31 I. Calvez, C. R. Szczepanski and V. Landry, Effect of Copolymer on the Wrinkle Structure Formation and Gloss of a Phase-Separated Ternary Free-Radical/Cationic Hybrid System for the Application of Self-Matting Coatings, *Polymers*, 2022, **14**, 2371.
32 H. Zhang and Z. Wu, Synthesis of epoxy-based silicone prepolymers with UV/moisture dual curability for applications in anti-graffiti coatings, *RSC Adv.*, 2022, **12**, 33945–33954.
33 F. Bian, X. Li, J. Zhao, X. Gui, J. Hu, S. Li and S. Lin, Synthesis of epoxy-based silicone prepolymers with UV/moisture dual curability for applications in anti-graffiti coatings, *React. Funct. Polym.*, 2022, **180**, 105396.
34 K. Suzuki and T. Ohzono, Wrinkles on a textile-embedded elastomer surface with highly variable friction, *Soft Matter*, 2016, **12**, 6176–6183.
35 M. Broxtermann and T. Jüstel, Photochemically induced deposition of protective alumina coatings onto UV emitting phosphors for Xe excimer discharge lamps, *Mater. Res. Bull.*, 2016, **80**, 249–255.
36 V. Petry and D. J. Kent, The effect of UV-curable formulations and matting agents on lacquer properties, *Surf. Coat. Int., Part B*, 2004, **87**, 103–109.
37 H. Ma, Y. B. Liu, J. B. Guo, T. B. Chai, S. B. Jing, Y. C. Zhou, L. D. Zhong and J. E. Deng, Synthesis of a novel silica modified environmentally friendly waterborne

polyurethane matting coating, *Prog. Org. Coat.*, 2020, **139**, 105441.

38 Y. Du, S. Shi, D. Jie, Z. Guo and L. Yong, Research on Light Scattering Effect of Calcined Diatomite Matting Agent in Coating Surface, *China Powder Sci. Technol.*, 2010, **16**, 31–33+44.

39 Y. Tsuzuki, Y. Oikubo, Y. Matsuura, K. Itatani and S. Koda, Vacuum ultraviolet irradiation on siliceous coatings on polycarbonate substrates, *J. Sol-Gel Sci. Technol.*, 2008, **47**, 131–139.

40 J. Ou, M. Zhang, H. Liu, L. Zhang and H. Pang, Matting films prepared from waterborne acrylic/micro-SiO2blends, *J. Appl. Polym. Sci.*, 2014, **13**, 132.

41 F. Bauer, R. Flyunt, K. Czihal, H. Langguth, R. Mehnert, R. Schubert and M. R. Buchmeiser, UV curing and matting of acrylate coatings reinforced by nano-silica and micro-corundum particles, *Prog. Org. Coat.*, 2007, **60**, 121–126.

42 F. Bauer, U. Decker, K. Czihal, R. Mehnert, C. Riedel, M. Riemschneider, R. Schubert and M. R. Buchmeiser, UV curing and matting of acrylate nanocomposite coatings by 172nm excimer irradiation, *Prog. Org. Coat.*, 2009, **64**, 474–481.

43 J. Y. Zhang, G. Windall and I. W. Boyd, UV curing of optical fibre coatings using excimer lamps, *Appl. Surf. Sci.*, 2002, **186**, 568–572.

44 H. Wang, S. Wang, X. Du, H. Wang, X. Cheng and Z. Du, Synthesis of a novel flame retardant based on DOPO derivatives and its application in waterborne polyurethane, *RSC Adv.*, 2019, **9**, 7411–7419.